

## Unbinding of Symmetric and Asymmetric Stacks of Membranes

Roland R. Netz and Reinhard Lipowsky

*Institut für Festkörperforschung, Forschungszentrum Jülich, 52425 Jülich, Germany*

(Received 20 July 1993)

The unbinding of  $N$  membranes interacting with attractive potentials is considered theoretically for zero pressure. In the *symmetric case*, for which the membranes have the same bending rigidity, all  $N$  membranes unbind simultaneously at the  $N$ -independent temperature  $T_c^s$  but with  $N$ -dependent effective critical exponents. In the *asymmetric case*, for which the lowest membrane acts as a rigid wall, they exhibit a sequence of unbinding transitions with universal exponents; the transition temperature of the uppermost membrane for a semi-infinite stack ( $N = \infty$ ) is again given by  $T_c^s$ .

PACS numbers: 82.70.-y, 64.60.-i

Lipid bilayers in aqueous solutions often form multilayer systems consisting of well-aligned membrane stacks. Bulk samples of such multilayer systems have been experimentally studied for a long time, primarily by x-ray diffraction [1]. It is also possible, however, to observe stacks consisting of a relatively small number of bilayers. This can be done by optical microscopy for freely suspended stacks [2] or by surface reflectivity measurements for bilayers which have been immobilized onto an interface [3].

The adhesion of the bilayers within the stack is governed by attractive van der Waals forces. These forces are renormalized by thermally excited shape fluctuations which act to reduce the adhesion energy [4]. This renormalization can be understood in a qualitative way if one considers the competition between the van der Waals attraction and the loss of entropy arising from the confinement of the membranes [5]. A more systematic treatment of this competition led to the theoretical prediction of a critical unbinding transition between bound and unbound membrane states [6] which has been observed experimentally for stacks of six to eight sugar-lipid membranes [7]. All membranes of these stacks appeared to be quite flexible and to have the same bending rigidity. The experimentally observed transitions were reversible and showed no hysteresis. In addition, the dependence of the unbinding temperature on the number of the membranes was found to be very weak.

In this Letter, we theoretically study the adhesion and unbinding of  $N \geq 2$  fluid membranes. We distinguish two different types of stacks which we call "symmetric" and "asymmetric." First, consider the symmetric case, for which all  $N$  membranes have the same bending rigidity and interact via identical potentials, which should apply to the stacks of sugar-lipid membranes as studied experimentally by Helfrich and co-workers [2,7]. In this case, we find that all  $N$  membranes unbind *simultaneously* at the  $N$ -independent temperature

$$T_c^s(N) = T_c^s. \quad (1)$$

However, we also find that the effective critical exponents for the unbinding transition depend on  $N$  and thus are nonuniversal over the accessible range of length scales.

This is in marked contrast to other theoretical work, as will be discussed below.

Next, consider an asymmetric stack, for which  $N - 1$  identical membranes are bound towards a rigid wall (labeled by  $n = 0$ ). This corresponds, e.g., to a stack of bilayers which has been immobilized on a glass slide [8] or at a liquid-vapor interface [3]. In this case, we find a *sequence* of unbinding temperatures  $T_c^a(n)$ . These temperatures must satisfy the inequalities  $T_c^a(1) \geq T_c^a(n) \geq T_c^a(\infty)$ . In fact, the unbinding temperature of the  $n$ th membrane is found to satisfy the relation

$$1 - [T_c^a(\infty)/T_c^a(n)]^2 \sim 1/n^\lambda \quad (2)$$

in the continuum limit with  $\lambda = 2.0 \pm 0.2$  and

$$T_c^a(\infty) = T_c^a(1)/\sqrt{2} = T_c^s. \quad (3)$$

Here, all unbinding transitions exhibit the same universal critical exponents. Thus, the mean separation  $\langle \delta l_n \rangle$  behaves as  $\langle \delta l_n \rangle \sim [T_c^a(n) - T]^{-\psi}$  with  $\psi = 1$ . It then follows from (2) that a semi-infinite stack at  $T = T_c^s$  is characterized by the self-similar density profile  $\rho(z) \sim z^{-\mu}$  where  $z$  denotes the distance from the rigid wall and  $\mu = \lambda\psi/(1 + \lambda\psi) \simeq 2/3$ .

Our approach is twofold: First, we apply standard Monte Carlo (MC) techniques to stacks of  $N$  two-dimensional membranes; the enormous numerical expense of these simulations restricts the number of membranes to  $N \leq 3$ . Second, we perform transfer matrix (TM) calculations for bundles of  $N$  one-dimensional strings (or stretched polymers); here, we are able to consider symmetric and asymmetric systems with  $N \leq 4$ . Renormalization group arguments predict the critical behavior to be analogous for strings and membranes [4,9]. This is confirmed by our analysis for  $N \leq 3$  and will be assumed to hold for general  $N$ . Extrapolation of our results to large  $N$  leads to (1)–(3).

The effective Hamiltonian for  $N$  manifolds is given by

$$\mathcal{H}\{l_N\} = \int d^q x \left\{ \sum_{n=0}^{N-1} \frac{K_n}{2} (\nabla^q l_n)^2 + \sum_{n=0}^{N-2} V(l_{n+1} - l_n) \right\}, \quad (4)$$

with  $q = 1$  and  $2$  for strings and membranes, respec-

tively. The manifolds are, on average, parallel to each other and parametrized by single-valued functions  $l_n(x)$ ; the statistical weight of a configuration  $\{l_N\}$  is given by the Boltzmann factor  $\exp(-\mathcal{H}\{l_N\}/T)$ . The positive constants  $K_n$ , which are the line stiffnesses and bending rigidities for  $q = 1, 2$ , respectively, have the values

$$K_n = K \quad \text{for } n = 0, \dots, N-1 \quad (5)$$

in the symmetric case and

$$K_n = \begin{cases} \infty & \text{for } n = 0, \\ K & \text{for } n = 1, \dots, N-1 \end{cases} \quad (6)$$

in the asymmetric case, where  $K_0 = \infty$  corresponds to the rigid wall. The interactions are defined by

$$V(l) = \begin{cases} \infty & \text{for } l \leq 0, \\ V^0 & \text{for } 0 < l < l^0, \\ 0 & \text{for } l^0 \leq l, \end{cases} \quad (7)$$

with  $V^0 < 0$  for an attractive potential well. Renormalization group calculations show that interactions which decay faster than  $\sim 1/l^2$  are all mapped onto one fixed point and thus give rise to identical critical unbinding behavior [10]. Since the van der Waals attraction between two membranes behaves as  $\sim 1/l^4$  for large  $l$ , the universal properties can be studied using the interaction (7).

Most of the interesting physics is caused by the non-crossing constraint, i.e.,  $l_0 < l_1 < \dots < l_{N-1}$  in (4), which is embodied via the hard wall at zero separation in (7). For our numerical studies, the center-of-mass coordinate, which diffuses freely, has been separated off. We also discretize the coordinate  $x$  with lattice constant  $a$  and use periodic boundary conditions in order to suppress edge effects; the problem defined by (4) then depends only on the rescaled potential depth  $U \equiv -a^q V^0 / T$  and on the rescaled potential range  $\tilde{l}^0 \equiv l^0 \sqrt{K/2Ta^q}$ .

In our calculations, we measured the mean separations between manifolds  $\langle \delta l_n \rangle \equiv \langle l_n - l_{n-1} \rangle$ , and the corresponding perpendicular and parallel correlation lengths,  $\xi_{\perp n}$  and  $\xi_{\parallel n}$ . The separations are expected to scale as

$$\langle \delta l_n \rangle - \langle \delta l_n(U = \infty) \rangle \sim (U - U_c)^{-\psi}, \quad (8)$$

and similarly  $\xi_{\perp n}$  and  $\xi_{\parallel n}$  with exponents  $\nu_{\perp}$  and  $\nu_{\parallel}$ , respectively;  $\langle \delta l_n(U = \infty) \rangle = \tilde{l}^0/2$  represents a correction to scaling. For direct comparability, we always set  $\tilde{l}^0 = 1$ , i.e., separations  $\langle \delta l_n \rangle$  are measured in units of  $\tilde{l}^0$ .

For the MC simulations, a square lattice consisting of 3920 discrete sites is partitioned into five sublattices; each sublattice is updated independently using a fully vectorized code employing the standard Metropolis algorithm [11]. In most runs, we did  $\simeq 10^7$  MC steps per site, which gives a statistical error of less than 1%. The rescaled range was always set to  $\tilde{l}^0 = 0.0185$ .

In Fig. 1, we show results for the asymmetric sys-

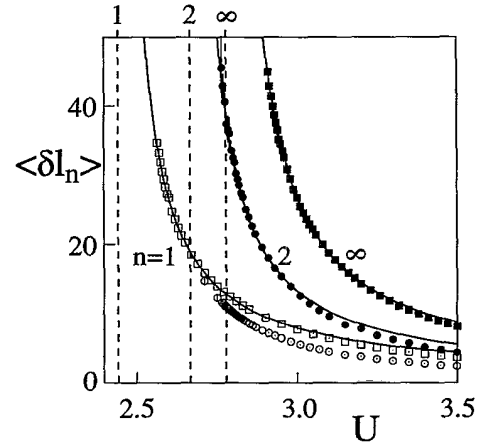


FIG. 1. Asymmetric stack of membranes: Monte Carlo data for the mean membrane separations  $\langle \delta l_n \rangle$  as a function of the potential strength  $U$ ; numerical errors are denoted by vertical lines.

tem of membranes bound to a rigid wall;  $\langle \delta l_1 \rangle$  and  $\langle \delta l_2 \rangle$  for  $N = 3$  (open and closed circles, respectively) clearly diverge at two different critical potential strengths  $U_c^a(n=1)$  and  $U_c^a(n=2)$ . Below  $U_c^a(2)$ , the values of  $\langle \delta l_1 \rangle$  obtained for  $N = 3$  equal the ones obtained for  $N = 2$  (denoted by open squares) as expected: After the unbinding of the upper membrane of an asymmetric  $N$  stack, the problem reduces to a stack of  $N-1$  membranes. Above  $U_c^a(2)$ , the upper membrane pushes the lower membrane closer to the wall, as can be seen from the difference between  $\langle \delta l_1 \rangle$  for  $N = 2$  and  $N = 3$ ; it exerts a *pressure* on the lower membrane. By fitting  $\langle \delta l_1 \rangle$  for  $N = 2$  and  $\langle \delta l_2 \rangle$  for  $N = 3$  to the form (8) we obtain  $U_c^a(1) = 2.44 \pm 0.01$  with  $\psi = 0.99 \pm 0.03$  and  $U_c^a(2) = 2.67 \pm 0.03$  with  $\psi = 1.0 \pm 0.2$ . This confirms the expectation that each unbinding transition is characterized by the universal exponent  $\psi = 1$ , as for two membranes. The solid curves in Fig. 1 correspond to the fits; the broken lines denote the obtained critical potential strengths.

Also shown in Fig. 1 is the variation of the separation for the case of two identical membranes (denoted by  $n = \infty$  as explained below); here we obtain  $U_c^s(N=2) = 2.78 \pm 0.01$  and  $\psi = 0.99 \pm 0.05$ . For three identical membranes we obtain  $U_c^s(N=3) = 2.785 \pm 0.01$  (as shown in Fig. 3). The two potential strengths are the same within the numerical error, thus suggesting that

$$U_c^s(N) \equiv U_c^s. \quad (9)$$

For the transfer matrix calculations we also discretize the coordinates  $\{l_n\}$  with lattice constant  $\Delta l = \sqrt{K/2Ta}$  on a hypercubic lattice (except where noted otherwise); this has to be done in accord with several symmetry and area conserving constraints [12]. Here we iterate the transfer matrix corresponding to (4) in the so-called restricted solid-on-solid approximation until convergence to the stationary probability distribution is achieved. [9]

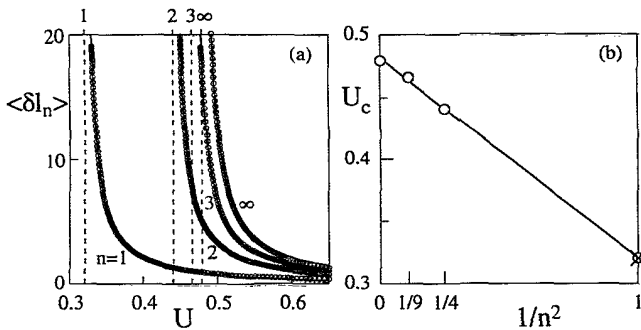


FIG. 2. Asymmetric bundle of strings: (a) Transfer matrix results for the mean string separations  $\langle \delta l_n \rangle$  as a function of the potential strength  $U$ . (b) Critical potential strengths (o) indicated by broken lines in (a) are shown together with an exact result (x).

In Fig. 2(a) we show our results for the unbinding of up to three strings from a rigid wall with  $n = N - 1$ ; here  $l^0 = 1/\sqrt{2}$ . As in Fig. 1, we denoted the unbinding of two identical manifolds by  $n = \infty$ ; here, we also calculated  $\langle \delta l_3 \rangle$  for the case  $N = 4$ . For a given value of the potential,  $\langle \delta l_i \rangle < \langle \delta l_j \rangle$  for  $i < j$ ; this indicates the effective flattening of the bound strings by the wall, which is mediated through the strings and becomes smaller for increasing  $n$ . The critical exponents for all four curves are given consistently by  $\psi = 1 \pm 0.02$ ; the critical potential strengths  $U_c^a$  are plotted in Fig. 2(b) as a function of  $1/n^2$ , which are well fitted by a straight line.

Both for membranes and for strings, our results for the critical potential strengths are described by the form

$$U_c^a(n) = U_c^a(\infty) - [U_c^a(\infty) - U_c^a(1)]/n^\lambda \quad (10)$$

with  $\lambda = 2.0 \pm 0.2$ . The equality  $U_c^a(n = \infty) = U_c^s$  follows from the expectation that the influence of the rigid wall on bound manifolds becomes weaker with increasing  $n$ ; thus, for large  $n$ , the  $n$ th manifold should unbind at a potential strength identical to the one found for symmetric stacks. This is indeed supported by the observation that the critical potential strength data in Fig. 2(b) extrapolate nicely to  $U_c^s$  for large  $n$ .

In the continuum limit of zero cutoff  $a$ , scaling shows that the set of parameters  $T, K, V^0$ , and  $l^0$  reduces to the combination  $v \equiv V^0 K (l^0/T)^2$ . In this limit, one finds  $U_c^a(\infty) = U_c^s = 2U_c^a(1)$  and obtains (2) and (3) using relation (10); this determines the temperature window for the unbinding transitions of the semi-infinite asymmetric stack. This window is reduced by the small-scale cutoff  $a$ : The larger the cutoff, the smaller the temperature window.

In Fig. 3 our MC results for a symmetric stack of three membranes are displayed. Here, due to the up-down symmetry, we expect (and indeed observe)  $\langle \delta l_1 \rangle = \langle \delta l_2 \rangle$  and use  $\langle \delta l \rangle \equiv \langle \delta l_1 \rangle/2 + \langle \delta l_2 \rangle/2$  (similarly for the other length scales). The parallel correlation length was estimated using  $\xi_{||} \equiv a \exp[2\pi \langle (\nabla \delta l)^2 \rangle / T]$  [11]. Figure 3(a)

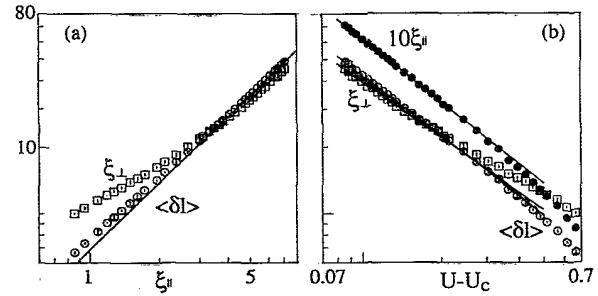


FIG. 3. Symmetric stack of three identical membranes: (a) Monte Carlo data for the membrane separation  $\langle \delta l \rangle$  and roughness  $\xi_{\perp}$  plotted against the parallel correlation length  $\xi_{||}$ . (b) All length scales plotted as a function of the reduced potential strength  $U - U_c$ ; the straight lines denote our fits.

shows the behavior of  $\langle \delta l \rangle$  and  $\xi_{\perp}$  vs the parallel correlation length on a log-log plot. The data tend toward the line with slope unity as one approaches the transition, indicating that  $\psi = \nu_{\perp} = \nu_{||}$  [13]. We fitted the data according to (8), obtaining  $U_c = 2.785 \pm 0.01$  and the effective exponents  $\psi = 0.91 \pm 0.04$ ,  $\nu_{\perp} = 0.83 \pm 0.10$ , and  $\nu_{||} = 0.93 \pm 0.06$ . In Fig. 3(b) we plot the data on a log-log scale, which shows that they scale rather nicely sufficiently close to the transition.

Figure 4 summarizes our TM results for the symmetric case with  $N = 2, 3$ , and 4, for which the discretization dictated  $l^0 = 1, \sqrt{3}/2$ , and  $\sqrt{2}$ , respectively. For  $N = 4$ , one has to distinguish between the outer separations, which are again related by the up-down symmetry, thus  $\langle \delta l_O \rangle \equiv \langle \delta l_1 \rangle/2 + \langle \delta l_3 \rangle/2$ , and the inner separation,  $\langle \delta l_I \rangle \equiv \langle \delta l_2 \rangle$ ; in principle, the unbinding process could now occur in two steps at distinct potential values. However, we find the two separations to diverge at exactly the same critical potential, namely  $U_c = 0.192 \pm 0.005$ ; the critical potential for the unbinding of two strings with  $l^0 = \sqrt{2}$  was found to be  $U_c = 0.193 \pm 0.005$  [12]; within

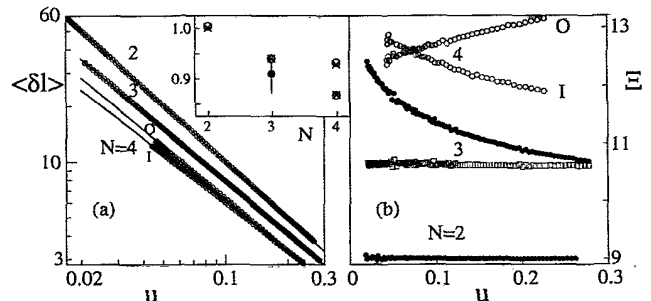


FIG. 4. Symmetric bundle of  $N$  strings: Transfer matrix results with the reduced potential strength  $u \equiv (U - U_c)/U_c$ . (a) The string separations  $\langle \delta l \rangle$  for  $N = 2, 3$ , and 4 scale with different exponents  $\psi$ , which are given in the inset (o) together with the exponents of the perpendicular correlation length  $\nu_{\perp}$  (x) and the MC estimate of  $\psi$  (•) for three membranes. (b) Extended analysis of the data shown in (a) using the quantity  $\Xi$  for the  $\langle \delta l \rangle$  data; see text.

the numerical error, they are identical. Three strings were found to unbind at the same  $U_c$  as two strings [12], therefore (9) is numerically confirmed for  $N \leq 4$ .

The observed universality in the critical potential depths is contrasted by an apparent nonuniversality in the effective exponents: In Fig. 4(a), we show our data for  $\langle \delta l \rangle$  in a log-log plot. For  $N = 2$  the data scale accurately with  $\psi = 1.005 \pm 0.005$ ; for  $N > 2$ , there are small but clear deviations from this universal value for the accessible length scales. Moreover, the inner and outer separations in the case of four strings are found to scale differently, giving  $\psi_O = \nu_{LO} = 0.93 \pm 0.02$  and  $\psi_I = \nu_{LI} = 0.87 \pm 0.02$ . In the inset, the values of  $\psi$  (circles) and  $\nu_{\perp}$  (crosses) are plotted as a function of  $N$ ; the MC result for  $\psi$  obtained for three membranes is also included (filled circle).

A rather accurate asymptotic analysis is possible using the quantity

$$\Xi[F] \equiv [F(U + \Delta U)^{-1/\gamma'} - F(U)^{-1/\gamma'}]/\Delta U. \quad (11)$$

Assuming the function  $F(U)$  to be of the form  $F(U) \approx b(U - U_c)^{-\gamma}$ , we get  $\Xi \approx (\gamma/\gamma')(U - U_c)^{\gamma/\gamma' - 1} b^{-1/\gamma'}$  for small  $\Delta U$ . For  $\gamma/\gamma' = 1$  this expression reduces to  $\Xi = \text{const}$ . For  $\gamma/\gamma' < 1$  and  $\gamma/\gamma' > 1$ ,  $\Xi$  diverges and approaches zero, respectively, as  $U$  tends towards  $U_c$ .

In Fig. 4(b), we show  $\Xi[\langle \delta l \rangle]$  for  $N = 2$  and 3 with  $\psi' = 1$  (solid circles); the divergence for  $N = 3$  indicates that  $\psi < 1$ . Indeed, plotting  $\Xi$  for  $N = 3$  with  $\psi' = 0.94$  (squares), we obtain a rather straight line over the whole accessible  $U$  range, indicating no crossover in the effective exponent as one approaches the transition. For  $\langle \delta l_O \rangle$  and  $\langle \delta l_I \rangle$  for  $N = 4$ ,  $\Xi$  is calculated with  $\psi' = 0.9$ , which lies in between the values obtained for the two exponents  $\psi_O$  and  $\psi_I$ . As shown in Fig. 4(b) for the inner (outer) separation,  $\Xi$  goes to infinity (zero) as  $U$  goes to  $U_c$ , indicating that the corresponding exponent is smaller (greater) than 0.9. Thus, over the accessible range of length scales, our data show that the effective critical exponents for the symmetric case depend on  $N$ . Critical behavior with  $N$ -dependent singularities has also been found for the necklace model which predicts, however, discontinuous transitions for  $N \geq 3$  [14] whereas we find continuous transitions for  $N = 3$  and  $N = 4$ . Likewise, our results disagree with the prediction of mean-field theories [15,16] and with the behavior of related, but somewhat different models [17,18] which exhibit  $N$ -independent critical exponents. In principle, the critical behavior as found here could be changed on sufficiently large length scales which are not accessible to our numerical methods. However, as far as the transition temperatures are concerned, such a crossover would not affect (1) and (3) and should have a rather small effect on (2).

In summary, it was shown (i) that a symmetric stack of  $N$  membranes unbinds at the transition temperature  $T = T_c^s$  which is independent of  $N$ , but exhibits  $N$ -dependent effective critical exponents over the accessible range of length scales; and (ii) that an asymmetric stack leads to a sequence of unbinding transitions at  $T = T_c^a(n)$ , see (2), which all belong to the same universality class.

The difference in the behavior of asymmetric and symmetric stacks should be observable in experiments on bilayer systems [19]. In fact, the universality of the transition temperatures for symmetric stacks is in agreement with experimental results for sugar-lipid membranes. [7]

We thank Willi Fenzl, Christin Hiergeist, and Michael Lässig for helpful discussions and acknowledge support by the Höchstleistungs-Rechenzentrum of the Forschungszentrum Jülich.

- [1] See, e.g., V.A. Parsegian, N. Fuller, and R.P. Rand, Proc. Natl. Acad. Sci. U.S.A. **76**, 2750 (1979).
- [2] W. Harbich and W. Helfrich, Chem. Phys. Lipids **36**, 39 (1984).
- [3] G. Cevc, W. Fenzl, and L. Sigl, Science **249**, 1161 (1990).
- [4] For a recent review, see R. Lipowsky, Physica (Amsterdam) **194A**, 114 (1993).
- [5] W. Helfrich, Z. Naturforsch. **33a**, 305 (1978)
- [6] R. Lipowsky and S. Leibler, Phys. Rev. Lett. **56**, 2541 (1986).
- [7] W. Helfrich and M. Mutz, in *Random Fluctuations and Growth*, edited by H.E. Stanley and N. Ostrowsky (Kluwer, Dordrecht, 1988); M. Mutz and W. Helfrich, Phys. Rev. Lett. **62**, 2881 (1989).
- [8] Such a system is often used for the preparation of vesicles, see D.D. Lasic, Biochem. J. **256**, 1 (1988).
- [9] R.R. Netz and R. Lipowsky, Phys. Rev. E **47**, 3039 (1993).
- [10] R. Lipowsky, Europhys. Lett. **7**, 255 (1988); Phys. Scr. **T29**, 259 (1989).
- [11] R. Lipowsky and B. Zielinska, Phys. Rev. Lett. **62**, 1572 (1989).
- [12] R.R. Netz and R. Lipowsky, J. Phys. I (France) (to be published).
- [13] J. Cook-Röder and R. Lipowsky, Europhys. Lett. **18**, 433 (1992).
- [14] D.A. Huse and M.E. Fisher, Phys. Rev. B **29**, 239 (1984).
- [15] S.T. Milner and D. Roux, J. Phys. I (France) **2**, 1741 (1992).
- [16] W. Helfrich, J. Phys. II (France) **3**, 385 (1993).
- [17] T.W. Burkhardt and P. Schlottmann, J. Phys. A **26**, L501 (1993).
- [18] C. Hiergeist, M. Lässig, and R. Lipowsky (to be published).
- [19] Our results also apply to wandering steps on vicinal surfaces or domain walls in adsorbed monolayers.